STRUCTURAL AND OPTICAL BEHAVIOUR OF DOPED TIN OXIDE NANOPARTICLES

T. Regin Das[1, 2] M. Meena[3*]

[1] Department of Physics, Lekshmipuram College of Arts and Science, Neyyoor, Affiliated to Manonmaniam Sundaranar University, Abishekapatti, Tirunelveli-627012, India. Email: regindphysics@gmail.com

[2] Research Scholar, Reg. No. 18223152131018, Department of Physics, S.T. Hindu College, Nagercoil, Affiliated to Manonmaniam Sundaranar University, Abishekapatti, Tirunelveli-627012, India

[3] Department of Physics, S.T. Hindu College, Nagercoil, Affiliated to Manonmaniam Sundaranar University, Abishekapatti, Tirunelveli-627012, India.

[*]Corresponding Author Email: meenaraj19@gmail.com

Abstract

Metal oxides have a lot of potential as a basic material for new technologies. Nano sized SnO_2, as a rutile structure semiconductor material with wide band gap of 3.6 eV, has many advantages, such as high theoretical capacity of 782 mAh/g, high density, clean and environmental protection, low cost, excellent cycling performance and excellent compactness performance. Low electrocatalytic efficiency of SnO_2 nano particle limits its use in many fields. To overcome this challenge, in our present work, we attempted to prepare nickel (Ni) and neodymium (Nd) doped SnO_2 Nano particles by simple cost effective hydrothermal method. A number of measures like X-ray diffraction (XRD), UV- absorption, Scanning electron microscope (SEM), and Transmission electron microscope (TEM) were used to explore their structure and physicochemical properties. SnO_2 crystallites were found to exhibit tetragonal rutile structure with average particle size of 24.1 nm. It was also established that the dopants Ni and Nd metal ions were successfully incorporated into SnO_2 without any structural changes in the host material. Doping of Ni and Nd metal ions results in a significant reduction in particle size and optical band gap. Electrochemical Impedance Spectroscopy (EIS) analysis was used to analyze the effect of dopants on the electrochemical behaviour of SnO_2. The results established that, presence of dopant reduces the electron-hole pair recombination and thus suggest the suitability of doped samples for photo-voltaic applications.

Keywords: Metal Oxides, Impedance spectroscopy, dopants, Recombination, luminescence etc

I. INTRODUCTION

Semiconducting metal oxide nanomaterials(SMO) are a prominent materials for scientific and technological advancement in nanoelectronics, optoelectronics, photovoltaics, magneto-optics, magneto-electronics, and photonic devices. These materials act differently than bulk semiconductors due to their distinct chemical, physical, electrical, and magnetic properties. In ongoing past SMO turns out to be exceptionally cutthroat material on account of their primary adaptability, synthetic soundness and the compactability with various biomolecules. World energy utilization to a great extent depends on the ignition of petroleum derivatives. In any case, the conventional way is neither reasonable nor earth harmless. Sustainable energy storage gadgets, like solar cells, thermoelectronic gadgets, are generally researched to supplant non-renewable energy sources. SMO material play had a fundamental impact in creating novel energy age gadgets.

Tin oxide (SnO_2) is one such SMO with large band gap of 3.6 eV that has been widely employed in flat panel displays, solar cells, and gas sensors. SnO_2 has piqued the curiosity of researchers since it is a naturally non-stoichiometric prototype transparent conducting oxide. It has a high level of transparency in the visible range and a high level of reflectance in the infrared region [1, 2]. Nowadays dye sensitized Solar cells (DSCs) are investigated as a next generation energy device. Grätzel and his coworker invented a solar cell based on the ruthenium sensitizer adsorbed on nanoporous TiO_2 semiconductor film [3]. However, the charge separation ability of TiO_2-based DSC is suppressed by its low electron mobility (<1 cm^2 V^{-1} s^{-1}) resulting in a higher dark current [4]. In this way, to conquer these issues with respect to TiO_2-based DSCs, other high band gap semiconductors like ZnO, SnO_2, and CdS were examined as conceivable elective semiconductor materials. In spite of the fact that SnO_2 has promising electronic properties, for example, higher electron portability, it shows substandard execution because of recombination of infused electrons with energized dye molecules and redox types of electrolyte.

In order to tune the properties of SnO_2 to make it a suitable material for DSSC, in our present study we made an attempt to synthesis nickel (Ni) and neodymium (Nd) doped SnO_2 Nano particles by simple cost effective hydrothermal method.

II.   EXPERIMENTAL SECTION

To synthesize pure and doped SnO_2 NPs, a surfactant-free one-step hydrothermal technique is used. The calculated amount (4.51 gram) of stannous chloride ($SnCl_2.2H_2O$) was dissolved in 100 ml of pure distilled water which was the starting solution. Separately, a calculated amount (3.603 grams) of urea was dissolved in 100 ml of distilled water. The solutions were then thoroughly combined and stirred for 30 minutes. During the stirring of mixed solutions 1% Nickel Chloride ($NiCl_2$) is added for Ni doped NPs, 1% Neodymium Chloride ($NdCl_2$) is added for Nd doped SnO_2 NPs separately. During the stirring process, NaOH solution was added drop by drop until it reached a pH of 13. The light milky-colored solution was then transferred to a Borosil Pot and placed in a microwave oven. The oven was set on medium temperature for 30 minutes. After cooling, the finalized product was cleaned numerous times with distilled water and acetone to eliminate organic contaminants [5]. A off white colour powder was obtained for pure and Ni doped NPs and light brown coloured powder for Nd doped NPs. All as prepared samples were annealed at 200ºC

III.   CHARACTERIZATION TECHNIQUES

Structure and morphology of the annealed samples were analysed by PXRD, SEM and TEM analysis. UV–DRS spectroscopy was performed on the NPs using a Perkin Elmer Spectrophotometer in the wavelength range 200–800 nm to investigate the absorption band and optical band gap. Photoluminescence tests of the NPs (at wavelengths ranging from 390 to 600 nm) were also carried out to identify surface flaws as well as luminescence characteristics. Electro chemical impedance spectroscopy (EIS) was used to analyse the electronic behaviour of the proposed samples.

IV.   RESULTS AND DISCUSSION

A. XRD Analysis

Figure 1(A)depicts the XRD pattern of pure, Ni and Nd doped, SnO_2 NPs. The spectra of pure SnO_2 NPs clearly shows that all the diffraction peaks correspond to the tetragonal lattice of SnO_2 NPs and are also well matched with the JCPDS data(File No: 14-1445). The structure of SnO_2 NPs is not affected by the addition of Ni and Nd dopants[6] but the diffraction peaks were shifted towards the lower angle side (fig; 1B). This may be due to variations in lattice parameters caused by tensile/compressive stress on the lattice.

Table 1 shows calculated values of the average particle size, lattice parameters and cell volume for pure, Ni and Nd doped SnO_2 NPs. Added dopants reduces the average crystallite size .reduction in crystallite size with Ni addition was reported by Bouras et al [7] owing to the smaller ionic radius of Ni (0.069 nm) than (0.071nm for Sn). It was also discovered that the unit cell volume of Nd doped SnO_2 is greater (71.584 $Å^3$). Because the ionic radius of Nd^{3+} (0.11 nm) is greater than that of Sn^{4+} (0.071 nm), integrating Nd^{3+} ions into the matrix is expected to cause some distortion and stress in the cell and lattice[8].

Reduction in particle size, increases the surface area of doped Nano particles when compared with pure SnO_2, hence increasing the dye adsorption nature of doped samples. This is an exceptionally certain commitment to upgrade gadget performance. Then again, the lower particle size additionally prompts expanded spilling of electrons from the semiconductor to recombine either with the redox species or with the oxidized dye atoms [9].

Table 1: Lattice parameters for pure and doped Nanoparticles

Sample	Pure SnO_2	Ni doped SnO_2	Nd doped SnO_2
Crystalline size (nm)	24.2	13.8	18.6
a=b (Å)	4.7373	4.7367	4.7383
c (Å)	3.1864	3.1848	3.1884
Cell volume (Å^3)	71.509	71.455	71.584
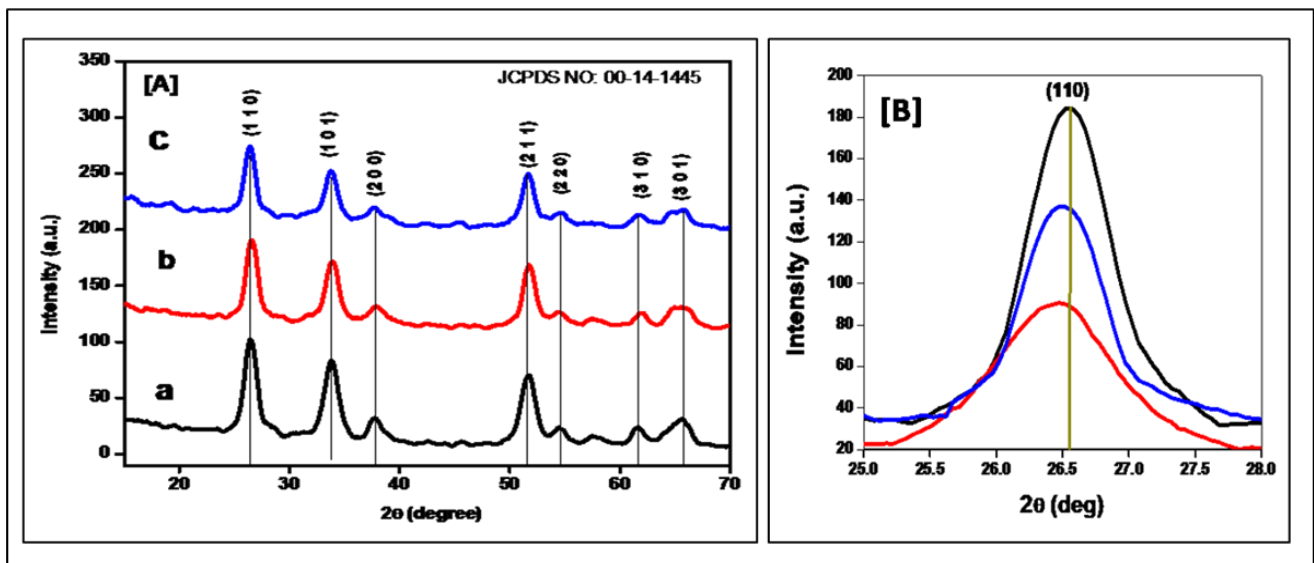
Fig 1: (A) XRD Pattern & (B)Corresponding shift in peaks of (a) pure SnO_2 NPs, (b) Ni doped SnO_2 NPs, (c) Nd doped SnO_2 NPs.

B. UV–Vis spectral analysis

UV–vis spectroscopy is an effective method for determining optical absorbance qualities and optical band gaps in materials. The material's optical characteristics reveal information on the energy band structure, impurity levels, excitons, localised defects, lattice vibrations, and specific magnetic excitations [10]. The optical band gap can be calculated using Tauc's plot by the relation[11].

$$\alpha h\upsilon = A(h\upsilon - E_g)^n$$

where α - absorption coefficient, h - Planck's constant, A - constant for a direct transition, ν - frequency of the incident photon, Eg band gap energy and n corresponds to the type of transition occur.

Figure 2(A&B) depicts the absorption spectra and tauc plot for the proposed samples. Pure, Ni doped, and Nd doped NPs have band gaps of 3.32eV, 2.43eVand 2.66eV respectively. The band gap of pure SnO_2 is reduced by the addition of dopants. The incorporation of dopant ions into SnO_2 may result in the introduction of defective energy levels into the band gap of SnO_2. This results in the formation of new lower energy electron-hole pair recombination centers in the energy gap of SnO_2 NPs and the shrinking of the SnO_2 band gap [6]. The reduction in band gap shows that the samples have the capability for photocatalytic degradation of organic contaminants when exposed to UV light [12].
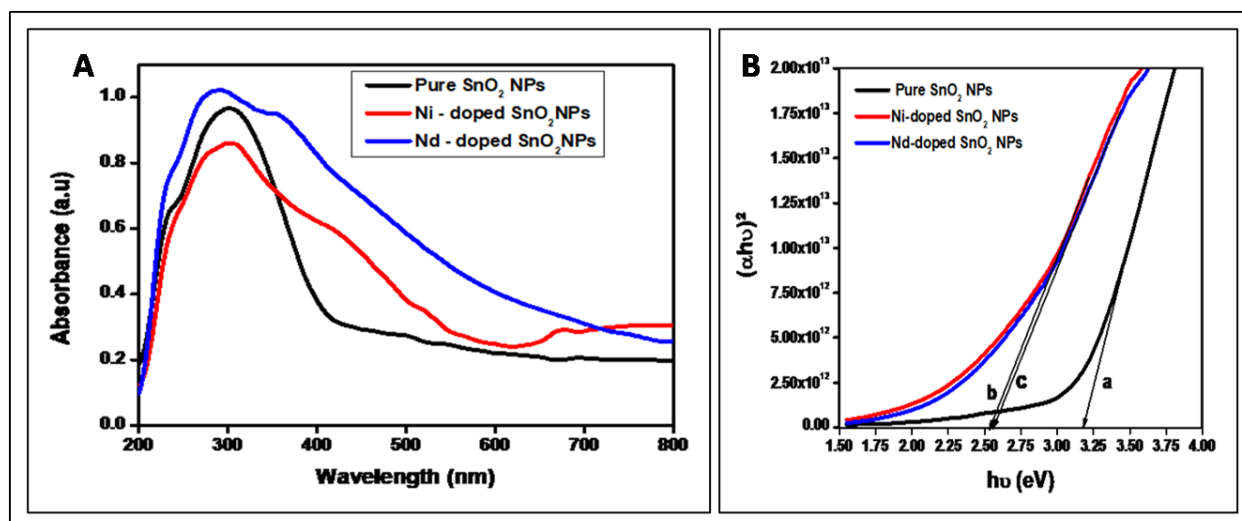
Figure 2: (A) UV – Absorption spectra and (B) tauc plot for pure and doped SnO₂ NPs

C. *Photoluminescence analysis*

The examination of photoluminescence (PL) is used to measure the purity, excitation energy, and crystalline quality of semiconductors and other functional materials. The PL feature does not exist in bulk SnO_2, but it occurs when the particle size approaches the nanometer level [13]. Changes in the exciton structure of the sample can be caused by transition metal doping. When the sample is doped with Ni, the oxygen vacancies increased due to the charge imbalance of Sn^{4+} and Ni^{2+}. As a result, a high number of free oxygen molecules can be adsorbed on the surface of nanoparticles [14]. The PL spectra of pure, Ni and Nd doped SnO_2 NPs are shown in Figure 3. The bands at 412 and 488 nm are formed by a radiative transfer of free electrons from intermediate donor levels caused by oxygen vacancies into valence band levels. The weak bands between 445 and 528 nm can be attributed to luminescent centers caused by inter-grain imperfections [15]. The creation of doubly charged oxygen vacancies may be responsible for the blue emission band near 456 nm [9]. At 505 nm, green emission is caused by the recombination of single oxygen vacancies in SnO_2 crystal lattices [16, 17].
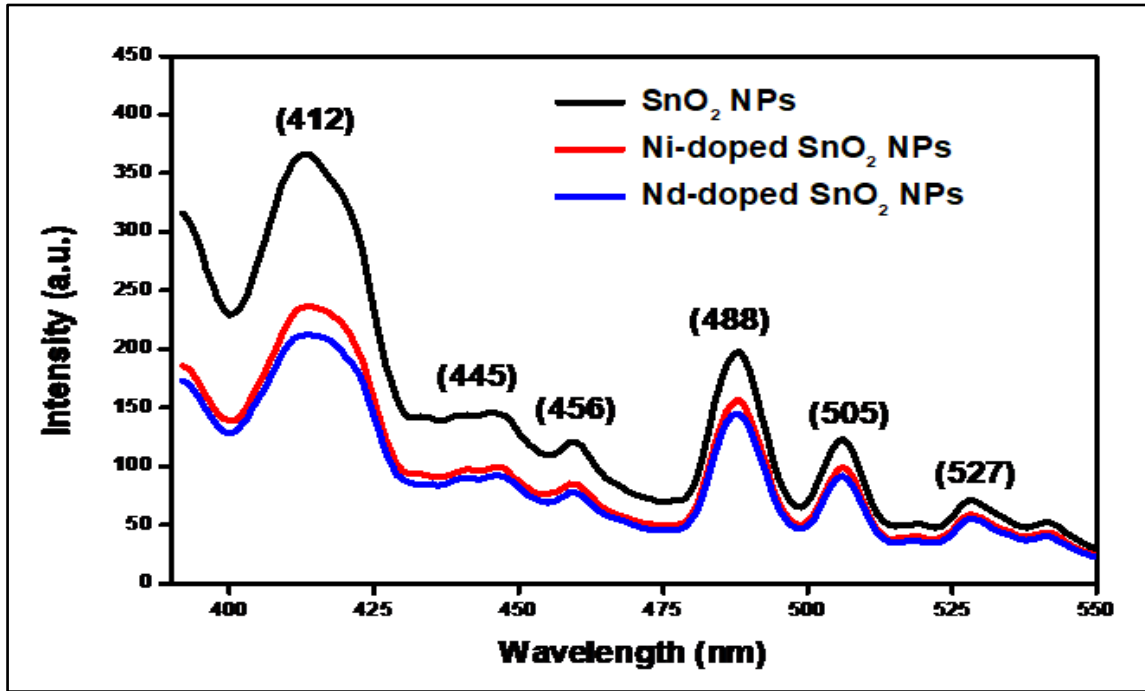
Figure 3: Photo luminescence spectra of pure and doped SnO₂ NPs

D. Surface morphology

Figure 4 shows TEM micrographs of pure, Ni doped and Nd doped SnO_2 NPs. All the samples are almost spherical in shape and agglomerated to reduce surface energy. TEM photos show that Ni and Nd do not produce any significant morphological changes in nanoparticles. The TEM was utilized to investigate the morphology and particle size further. Individual HR-TEM images show that the average particle size for pure, Ni, and Nd doped SnO_2 NPs is 15.20 nm, 7.93 nm, and 11.8 nm, respectively. The d-spacing of NPs was found to be 0.285, 0.364 and 0.264 nm, equivalent to (1 0 1), (1 1 0), and (1 0 1), respectively. The selected area electron diffraction pattern given in Fig 5(a-c) depicts the distinctive diffraction rings allocated to the crystal planes (1 1 0), (1 0 1), (2 0 0), (2 1 1), and (1 1 2) for pure, Ni, and Nd doped SnO_2 NPs . These values are consistent with the XRD data and show that the samples are polycrystalline. Ni and Nd atomic ratios were calculated to be 0.27 % and 1.91 %, respectively. The presence of Sn, O, Ni and Nd in the prepared samples is confirmed by EDAX analysis [Fig 5(d,e,f)]. The spectrum indicates that there are no extra contaminants in the processed samples.
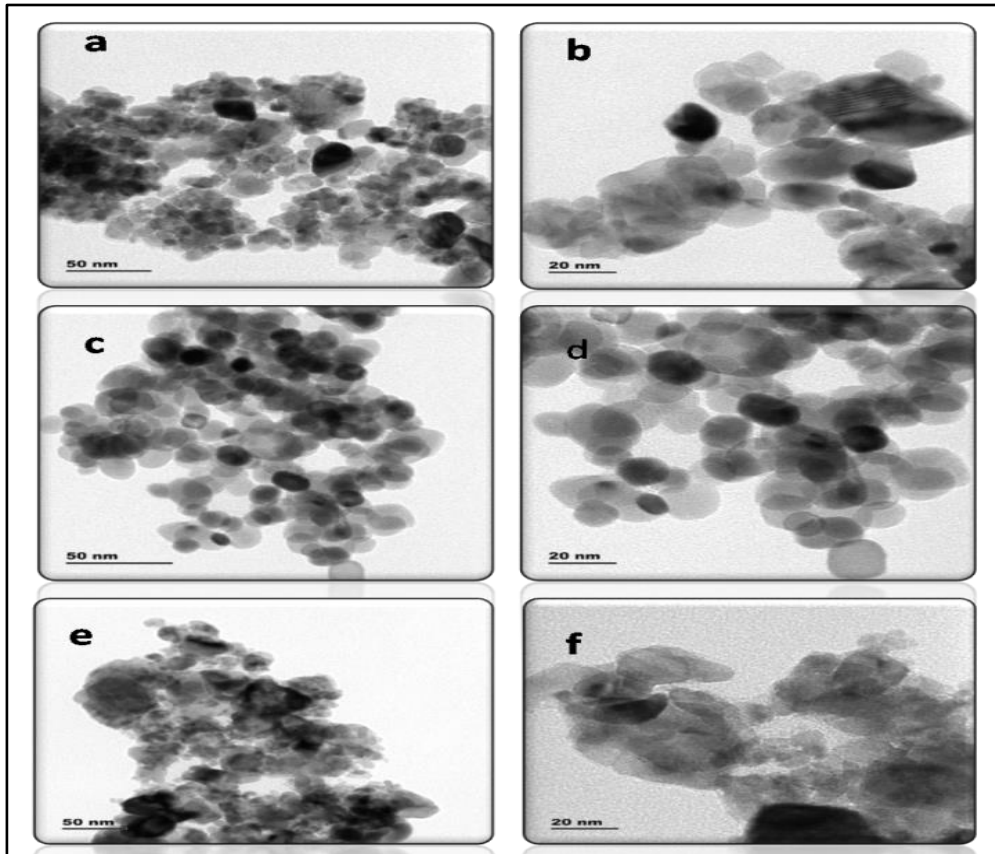
Fig 4: TEM images for (a,b) pure (c,d) Ni doped and (e,f) Nd doped SnO₂ NPs, (a,c,e) at 50 nm depth and (b,d,f) at 20 nm depth
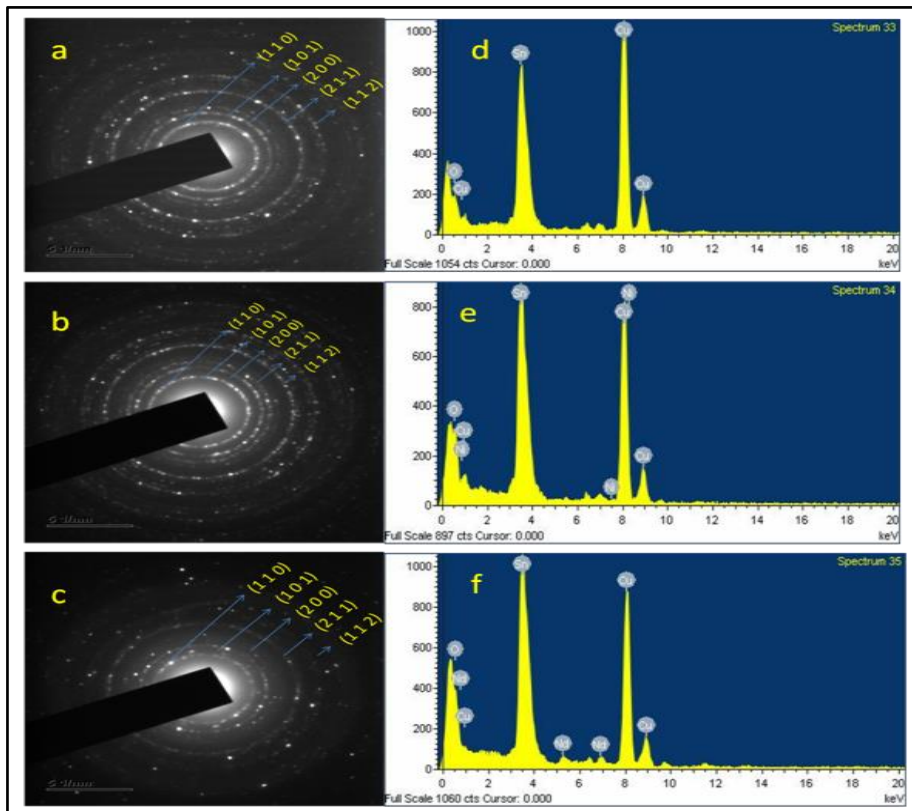
Fig 5: (a,b,c) SAED Pattern and (d,e,f) EDAX spectrum for (a,d) pure (b,e) Ni doped and (c,f) Nd doped SnO₂ NPs.

E. *Representations of Electrochemical impedance spectroscopy (EIS)*

One of the most significant electrochemical methods is Electrochemical Impedance Spectroscopy, which measures the impedance in a circuit in ohms. EIS has various benefits based on the fact that it is a steady-state approach, it employs small signal processing techniques, and that it can explore signal relaxations over a very large frequency range. The equivalent circuit model matched with Nyquist plot is given in fig 6.
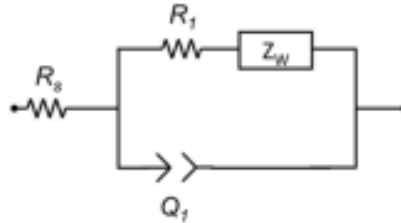
Fig 6: Equivalent circuit model of EIS technique

Where R_1 is the charge transfer resistance, Q_1 the double layer capacitance and Z_W Warburg diffusion, describes the impedance of diffusion and may be explained using finite and infinite diffusion models. The phrase Rs is used to account for all resistances connected with solution, cables, clips, and other components [18]. To analyze the electron transfer process, the charge transport resistance (R1) is determined at the electrode–electrolyte interface. R1 is determined by the electrode's dielectric and insulating properties. R1 is therefore a key variable in determining the efficiency of the coated electrode material in transferring charges from the solution to the electrode. Because metal doping improves charge transfer kinetics due to their increased conductivity, the inclusion of metal transition elements with SnO_2 is excellent for creating a better sensor response. Anodic and cathodic peak currents in the metal-doped nanocomposite were greater than in pure SnO_2 [19]. Additionally, doping the transition metal in SnO_2 frequently resulted in an abundance of surface oxygen vacancies, which adsorbs more oxygen molecules than ideal sites due to the lower adsorption energy of oxygen molecules at the vacant site [20]. Fig 7(a) reveals the EIS spectra of pure Ni and Nd doped SnO_2 NPs. The semicircular shape of the curves represents the charge transfer resistance. The charge transfer resistance of Ni and Nd doped samples are comparatively small with the pure SnO_2. This leads to the application in the solar cell devices. Figure 7(b) shows the variation of impedance ($\log Z_{img}$) with frequency. The AC electrical conductivity of pure Ni and Nd doped samples at 1 KHz frequency are 0.1963, 0.289 and 0.1993 mho cm^{-1} repectively. Ni doped sample perform better result than pure and Nd doped NPs.
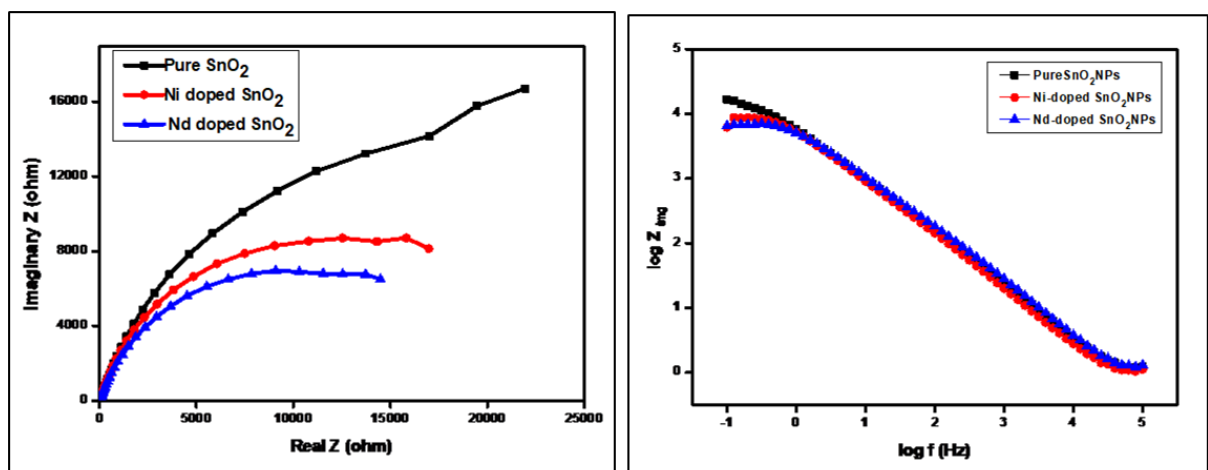
Fig 7: (a) Nyquist plot and (b) Bode magnitude plot for pure Ni and Nd doped SnO_2 nanoparticles

V. CONCLUSION

The nanoparticles were synthesized by simple hydrothermal method without the use of any special atmosphere. Characterizations revealed the purity and applicability of the synthesized samples. Small particle size and particle size uniformity are particularly notable for Ni doped SnO_2 NPs. Doping Ni and Nd reduces the band gap, allowing the doped samples to be used for photovoltaic and photocatalytic applications. As a result of the excitation from high energy states, significant photoluminescence characteristics in the near infrared region were detected for all samples. Observable performance is noted from the electrochemical impedance spectroscopic studies of Ni and Nd doped samples for solar cell applications.

VI. REFERENCES

1. V. Tadeev, G. Delabouglise, and M. Labeau, (1998), Influence of Pd and Pt additives on the microstructural and electrical properties of SnO_2-based sensors, Mater. Sci. Eng. B 5776.
2. D. P. Joseph, P. Renugambal, M. Saravanan, S. P. Raja, and C. Venkateswaran, (2009), Effect of Li doping on the structural, optical and electrical properties of spray deposited SnO_2 thin films, Thin Solid Films. 517, 6129-6136.
3. B. O.Regan and M. Grätzel, (1991), A low-cost, high-efficiency solar cell based on dye-sensitized colloidal TiO_2 films, Nature, vol. 353, 6346, 737–740.
4. K. Premaratne, G. R. A. Kumara, R. M. G. Rajapakse, and M. L. Karunarathne, (2012), Highly efficient, optically semi-transparent, ZnO-based dye-sensitized solar cells with Indoline D-358 as the dye, Journal of Photochemistry and Photobiology A: Chemistry, 229, 1, 29–32,.
5. R Sakthi Sudar Saravanan, M Meena, D Pukazhselvan and CK Mahadevan, (2015), Structural, optical and electrical characterization of Mn^{2+} and Cd^{2+} doped/co-doped PbS nanocrystals. J.Alloys and compounds, 62769-77.
6. Ateeq Ahmed, T. Ali,1 M. Naseem Siddique, Abid Ahmad, and P. Tripathi, (2017), Enhanced room temperature ferromagnetism in Ni doped SnO_2 nanoparticles: A comprehensive study, Journal of Applied Physics. 122, 083906.
7. K. Bouras, J.-L. Rehspringer, G. Schmerber, H. Rinnert, S. Colis and G. Ferblantie. (2014), Optical and structural properties of Nd doped SnO_2 powder fabricated by the sol–gel method. J. Mater. Chem. C. 2, 8235.
8. W. M. N. M. B. Wanninayake, K. Premaratne, G. R. A. Kumara, and R. M. G. Rajapakse, (2016), A study of the efficiency enhancement of the gel electrolyte-based SnO_2 dye-sensitized solar cells through the use of thin insulating layers, Electrochimica Acta, vol. 210, pp. 138–146.
9. P. Chetri, B. Saikia, and A. Choudhury, (2013), Structural and optical properties of Cu doped SnO_2 Nanoparticles, J. Appl. Phys. 113, 233514.
10. J. Jeyaram, K. Varadharajan, B. Singaram and R. Rajendhran, (2017), Optical, photoconducting, thermal and anisotropic mechanical behaviours of Benzimidazolium salicylate single crystals, J. Science Advanced Materials and devices. 2, 4, 445-454.
11. J. Tauc and A. Menth, (1972), States in the gap, J. Non-Cryst. Solids, 8-10, 569-585.
12. T. Amutha, M. Rameshbabu, S. Sasi Florence, N. Senthilkumar, I. Vetha Potheher and K. Prabha. (2019), Studies on structural and optical properties of pure and transition metals (Ni, Fe and co-doped Ni–Fe) doped tin oxide (SnO_2) nanoparticles for anti-microbial activity..Research on Chemical Intermediates, 45, 1929–1941.
13. Feng Jiang, Lizhi Peng and Tianfu Liu, (2020), Ni-Doped SnO_2 Dilute Magnetic Semiconductors: Morphological Characteristics and Optical and Magnetic Properties, J Superconductivity and Novel Magnetism, 33, 3051-3058.
14. Chetri. P, Choudhury.A and Choudhurym.B, (2014), Room temperature ferromagnetism in SnO_2 nanoparticles: an experimental and density functional study, A. J. Mater. Chem. C. 2(43), 9294–9302.
15. F. Gu, S.F. Wang, M.K. Lü, G.J. Zhou, D. Xu and D.R. Yuan, (2004) Photoluminescence properties of SnO_2 nanoparticles synthesized by solgel method, J. Phys. Chem. B, 108, 8119–8123.
16. K. Thirumurugan, K. Ravichandran, R. Mohan, S. Snega, S. Jothiramalingam and R. Chandramohan, (2013), Effect of solvent volume on properties of SnO_2, Surf Eng., 29(5), 373–378.

17. M.Ahmed, A. Bakry, E.ssam R. Shaaban and H. Dalir, (2021), Structure, Optical and electrical properties of Indium Tin Oxide thin films and their influence on performance of CdS/CdTe thin-film solar cells, J. Mater. Sci. 8, 11107-11118.
18. Hend S. Magar, Rabeay Y. A. Hassan and Ashok Mulchandani, (2021), Electrochemical Impedance Spectroscopy (EIS): Principles, Construction, and Biosensing Applications, Sensors, 21, 6578.
19. Upasana Choudhari and Shweta Jagtap, (2021), Electrochemical studies on doped SnO_2 nanocomposite for selective detection of lung cancer biomarkers, AIP Advances, 11, 125327.
20. Z. Jiang, R. Zhao, B. Sun, G. Nie, H. Ji, J. Lei, and C. Wang, (2016), Highly sensitive acetone sensor based on Eu-doped SnO_2 electrospun nanofibers, Ceram. Int, 42, 15881–15888.